

Optical Detection of Lesions in the Depth of a Solid Breast Phantom

Anett Bailleu, Axel Hagen, René Freyer
 Hochschule für Technik und Wirtschaft Berlin
 FB 1 – Energie und Information
 12459 Berlin, Germany
 e-mail: anett.bailleu@htw-berlin.de,
 axel.hagen@htw-berlin.de, renefreyer@gmx.net

Dirk Grosenick
 Physikalisch-Technische Bundesanstalt
 PTB Berlin
 10587 Berlin, Germany
 e-mail: dirk.grosenick@ptb.de

Abstract — In this study, a novel approach for optical imaging of tissue based on diffusely reflected photons was investigated. The examination object was an established solid breast phantom, which contains two absorbing lesions at different depths. The aim was to generate an absorption contrast image using depth discrimination to detect a lesion. The main questions was whether the required depth sensitivity is achievable with a near infrared line light source and a charge-coupled-device-camera. Different light sources were examined by comparative measurements. During the investigations observed speckle-effects could be reduced. The results of this study indicate that a translation of the approach from the breast phantom to in vivo studies appears feasible.

Keywords— near infrared remission; optical tomography; depth sensitivity.

I. INTRODUCTION

Diffuse optical imaging is a powerful tool to gain physiological and functional information from healthy and diseased tissue [1]. With near-infrared radiation in the 650 nm to 1000 nm wavelength range tissue concentrations of characteristic absorbers such as oxygenated and deoxygenated hemoglobin can be determined non-invasively. Main applications of diffuse optical imaging include the detection and characterization of tumors, e.g., in the female breast [2], functional studies on the human brain [3] - [5], as well as tissue oxygenation measurements in muscles [6], [7]. Furthermore, contrast agents offer the possibility to exploit molecular signatures for early detection of diseases [8] - [19].

A challenging task in diffuse optical imaging is to obtain either fully three-dimensional images of tissue regions with high spatial resolution or, at least, depth-resolved information about the distribution of tissue absorbers of interest. Accordingly, different techniques have been developed such as 3D tomographic imaging, oblique projection imaging in transmission, time-resolved or spatially resolved detection of reflectance, as well as laminar optical tomography [20] - [22].

Currently our research group, Labor Prozessmess- und Stelltechnik at the Hochschule für Technik und Wirtschaft Berlin (HTW Berlin, university of applied science) with

support from the Physikalisch-Technische Bundesanstalt Berlin (PTB, The National Metrology Institute of Germany), is developing a new procedure for near infrared (NIR) measurements [23] - [26], which has the potential to detect and depict changes in human tissue in a way suitable for medical diagnostics. This patented procedure [24] can complement and partly replace current radiologic imaging methods. This is desirable, since current technologies work with ionizing radiation and partly with radioactive markers (Scintigraphy-tracer), and therefore, additionally burden patients health.

Our proposed approach is a combination of two well-known methods: the light-section method (laser triangulation) [27] and the laminar optical tomography (LOT) [21], [22]. How it is possible to generate a 3D-scan by the light-section method in a very cost-effective way and how tomographic information of an examination object maybe combined with topographic information of the same object are subject-matters of other studies [23] - [26] and will not be described in this paper.

A. Aim of the Study

One of the most qualifying properties of the proposed procedure is the depth in which information can be obtained.

Fig. 1 shows a schematic representation of the LOT-principle. It depicts how to get optical information from inside of the examination object using a remission geometry.

A line generator and a light detector are placed at the same side of the examination object. The light source (a NIR-laser or NIR-light emission diode) projects a line on the surface of the examination object. A camera works as the light detector and takes images. The intensities of image-pixels in the vicinity of an “offset-line” are analyzed.

Measurements were carried out on an established solid-body phantom of a female breast in order to assess the depth sensitivity of the proposed procedure.

Extracted information of intrinsic absorbers from this mammary phantom are detected in both lateral and depth dimensions.

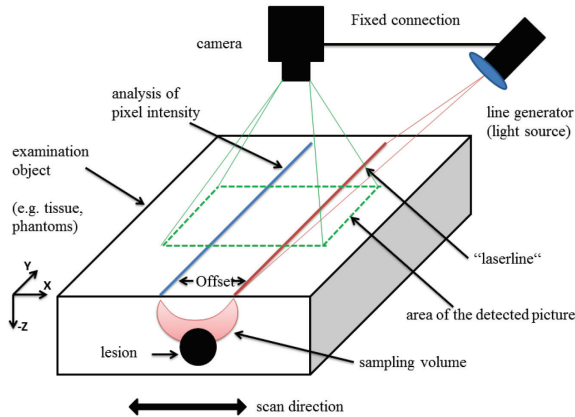


Figure 1. Principle to detect lesions in the sampled volume of a scattering examination object

B. Structure of the paper

The paper is divided into four main sections. Following the introduction in section 1, the section 2 contains a short description of the theoretical photon paths in a scattering medium as well as a description of the experimental setup and of the characteristics of the employed breast phantom. In section 3 measurement results are shown and interpreted. In section 4, the last one, we present a conclusion and an outlook into future work.

II. GENERATION OF DEPTH INFORMATION

The fundamentals of the investigation method are subdivided into a theoretical simulation and the experimental realization.

A. Theoretical Model

To gather information from the depth of a scattering medium, one possible approach is to have a local offset between the side where the photons enter the object and where they leave it. The possible depth resolution is dependent on this offset. The theoretical resolution can be estimated by solving the optical diffusion equation or by using Monte Carlo simulations of light transport.

Fig. 2 depicts simulation results for two different local offsets in remission geometry according to the photon diffusion model.

Photon bananas (i.e., banana formed curves in the diagram) are colored depending on the probability of photons passing this area.

The spread of the photon banana characterizes which optical differences inside the tissue can be detected through this measurement.

Additionally, Fig. 2 shows that under the assumed conditions, a depth resolution of about 1cm is to be expected [23].

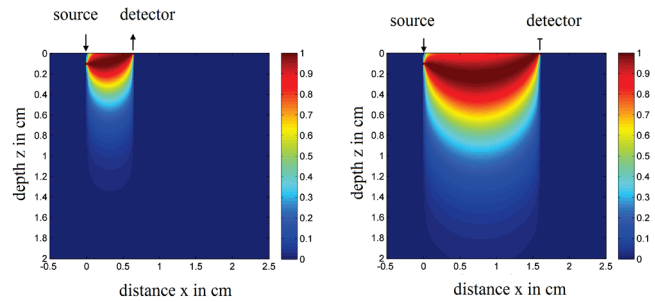


Figure 2. Photon "bananas" for two different offsets between source and detector position

B. Experimental Realization

1) Experimental Setup

Experiments were carried out with a remission geometry setup as depicted in Fig. 3 and Fig. 4. A camera is mounted perpendicular to the test object, which allows spatially-resolved detection of the diffusely reflected light.

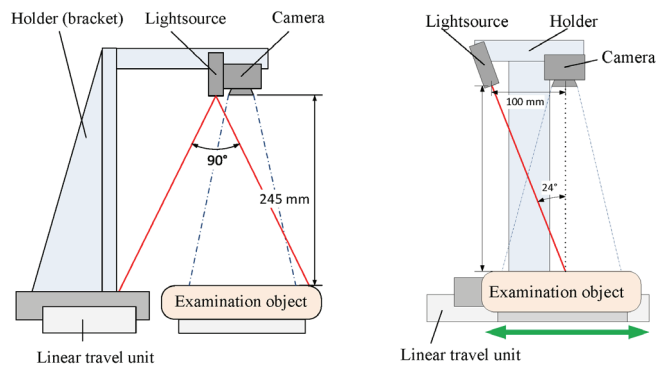


Figure 3. Scheme of the experimental setup

The line generator emits light with an angle of 24° with respect to the optical axis of the camera.

Light source and camera are mounted on a motorized translation stage and moved together over the examination object in a linear fashion.

Camera images were acquired with a step size of 1.25 mm using an exposure times of typically 4 ms to 10 ms.

A photographic image of the realized experimental setup is shown in Fig. 4. An industrial charge-coupled device (CCD) camera (Allied Vision Gruppy Pro F125) with enhanced NIR sensitivity and equipped with a high aperture c-mount objective [24] is employed as photon detector. The camera has a quantum efficiency of 24% in the wavelength range of 780-785nm, which was used for the experiments. Furthermore, the camera has a resolution of 1292x964 pixels.

The following light sources were investigated as possible line generators:

- a 785 nm high coherent continuous wave laser (cw-laser; Z-Laser Optoelektronik GmbH (DE): ZM18RF379 Z80M18S-F785-1g90),
- a 780 nm picosecond-pulsed laser (PsP; PicoQuant GmbH (DE): PDL 808 Sepia. + LDH-8-1-1097),
- a fiber coupled 780 nm incoherent high-power light emission diode (fiber-coupled LED; Thorlabs Inc. (US): M780F2).

To generate the line profile, each source was equipped with a broadband anti-reflection coated cylindrical lens.

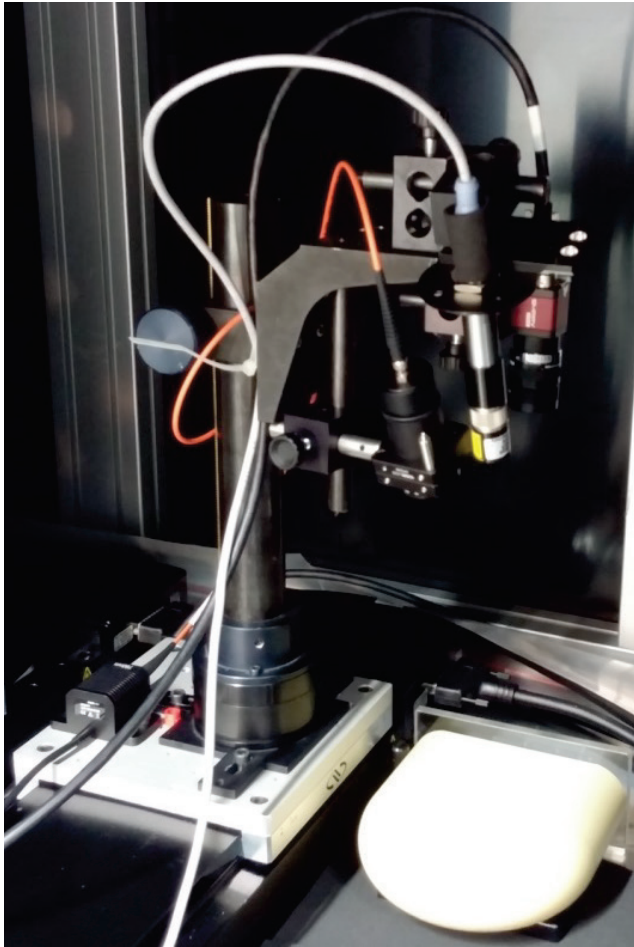


Figure 4. Photographic image of the experimental setup

2) Examination Object

We used an established phantom of the female breast provided by the Physikalisch-Technische Bundesanstalt Berlin (PTB the National Metrology Institute of Germany) as examination object (Fig. 5).

The phantom has two embedded spherical lesions with a diameter of 10 mm each (Fig. 5).

The center of the superficial lesion (lesion 1) is 10mm below the surface. The center of the second lesion (lesion 2)

is 25 mm below the surface. Accordingly, the top of the lesions is 5 mm respectively 20 mm below the surface.

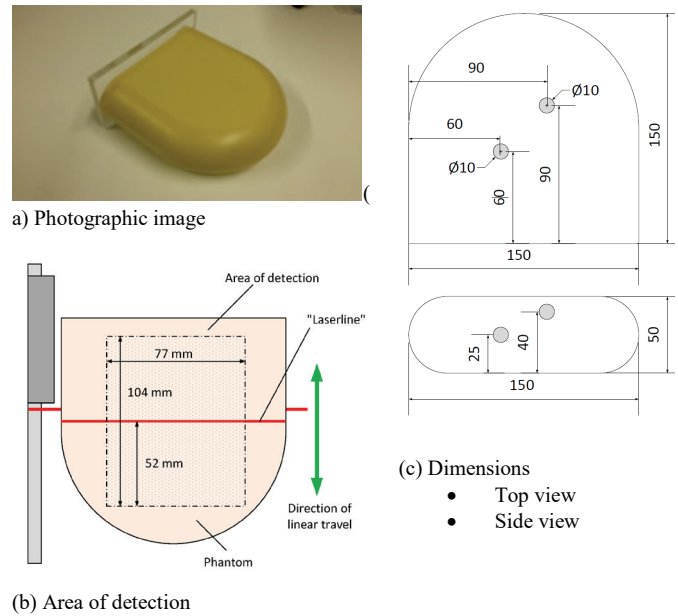


Figure 5. Solid-body-phantom of the female breast.

The optical properties of the phantom are:

- $\mu_a(\text{lesion 1}) = 0.17 \text{ cm}^{-1}$,
- $\mu_a(\text{lesion 2}) = 0.20 \text{ cm}^{-1}$,
- $\mu_s'(\text{lesion 1}) = 7.9 \text{ cm}^{-1}$,
- $\mu_s'(\text{lesion 2}) = 7.7 \text{ cm}^{-1}$,
- $\mu_a(\text{background}) = 0.043 \text{ cm}^{-1}$,
- $\mu_s'(\text{background}) = 8.3 \text{ cm}^{-1}$.

Both lesions exhibit roughly a 5-fold absorption-enrichment compared to the surrounding background.

III. RESULTS AND DISCUSSION

Fig. 6 depicts the normalized absorption images of a rectangular image section (Fig. 5b) of the phantom obtained with the different light sources (see 2.2.1). The superficial lesion is detectable with all three light sources; moreover its size can be estimated to a high degree.

In contrast to lesion 1, lesion 2 that is 25 mm below the surface cannot be seen in Fig. 7. Lesion 2 remains also hidden for higher offset values due to the limits in the dynamic range and in the signal-to-noise ratio.

From these result, we conclude, that the proposed procedure:

- Is suitable to detect inhomogeneities (e.g., lesions) in human tissue up to a depth of 1cm,
- is most likely not adequate to find inhomogeneities (e.g., lesions) in human tissue, which are deeper than 2cm under the surface of the skin.

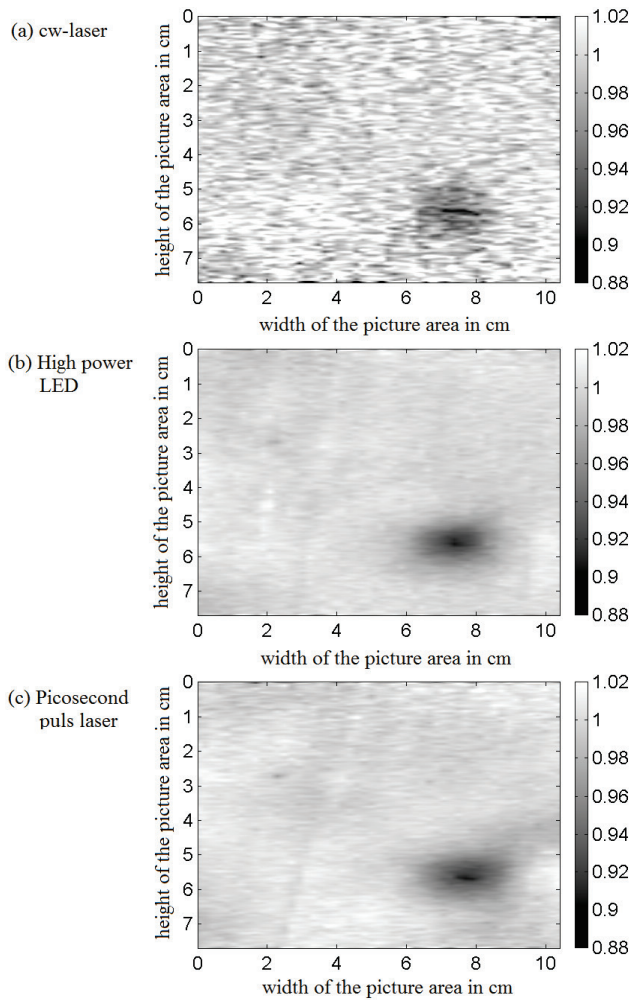


Figure 6. Detection of the lesion 1 in the phantom of a mammary

The objects in Fig. 6 show an oval-shaped distortion along the (horizontal) scan direction. As illustrated in Fig. 7, this effect is caused by the specific source-detector arrangement in our measurement. When moving source and detector with the fixed offset across a lesion, the propagation of photons is affected by the lesion two times, once for the light source and once for the detector being close to the lesion position (Fig. 7).

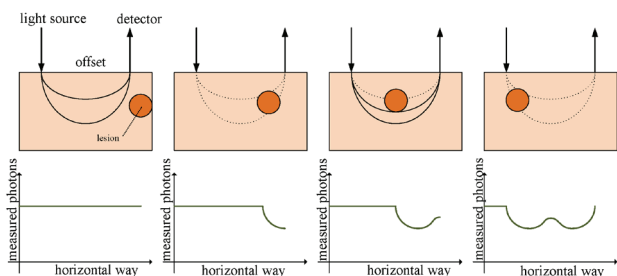


Figure 7. Horizontal distortion

The image quality obtained with the continuous-wave laser (cw-laser) source (Fig. 6a) is worse than with the other two light sources due to the speckle effect. When using the LED light source, this effect is not present due to the incoherent nature of its light. The speckle effect is also suppressed when applying the picosecond pulsed diode laser which has a much broader spectral width than the cw-laser.

The results of the high-power LED and the picosecond-pulse-laser are similar in overall quality. Since the picosecond-pulse-laser is more expensive and more complicated in usage, we conclude that the high-power LED is the best tested light source for practical application.

This perception is confirmed by calculation of the image contrast to noise ratio (CNR) for different experiments (Tables 1, 2).

The contrast is defined as the difference in signal intensity or gray-scale value between the side of the lesion and the side of ambient tissue. Dividing this value by the ambient noise (standard deviation, SD), the result is the contrast-to-noise ratio CNR. The used region of interests (ROI) to find the signal intensity S_A of the ambient tissue, the signal intensity S_L of the detected lesion and a range to calculate the standard deviation (SD, sigma) in this study are shown in Fig. 8.

The CNR is determined over the equation:

$$CNR = \frac{|S_L - S_A|}{SD} \quad (1)$$

S_L is the signal value at the center position of the detected lesion, while S_A is an average value and SD is the corresponding standard deviation of an ambient tissue are of $100 * 100$ pixels ($\approx 8 \text{ mm} * 8 \text{ mm}$).

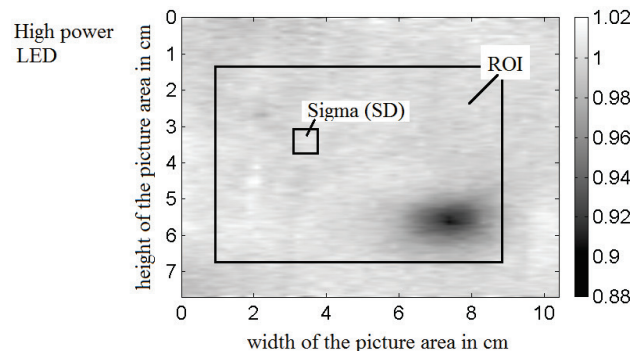


Figure 8. Special areas in the tomographic picture to calculate the contrast to noise ratio

The contrast to noise ratio in Fig. 6a (CNR = 14) is significantly worse rated than in Fig. 6b (CNR = 27) or Fig. 6c (CNR = 25).

Beside the kind of light source, other parameters have an effect to the CNR (Tables 1, 2):

- the applied power of the light source,
- the integration-time of the camera.

TABLE 1. COMPARISON OF CONTRAST TO NOISE RATIO VALUES BY USING THE LIGHT SOURCES IN A LOW INTENSITY MODE

Time of integration of the camera	CNR cw-laser	CNR High-power LED	CNR Picosecond pulse laser
4 ms	13	16	16
7 ms	16	22	23
10 ms	14	27	25

The general expectation is that both, an increase of the source power and an increase of the integration time of the detector, improve the CNR. But due to the speckle-effects the cw-laser produces better results in low intensity mode because the device goes below the laser threshold and acts mainly as an incoherent LED.

TABLE 2. COMPARISON OF CONTRAST TO NOISE RATIO VALUES BY USING THE LIGHT SOURCES IN A HIGH INTENSITY MODE

Time of integration of the camera	CNR cw-laser	CNR High-power LED	CNR Picosecond pulse laser
4 ms	10	26	26
7 ms	8	28	31
10 ms	10	33	33

With spatial averaging an additional improvement with respect to speckle-interferences can be achieved. (CNR = 64, Fig. 9).

This shows that even a coherent light source can produce a good contrast to noise ratio, if the speckle interference is eliminated. But even a CNR of 64 generated only limited additional value, i.e., the deeper positioned lesion 2 is still not detectable. Nonetheless with a higher CNR the edges of lesion 1 are less blurred.

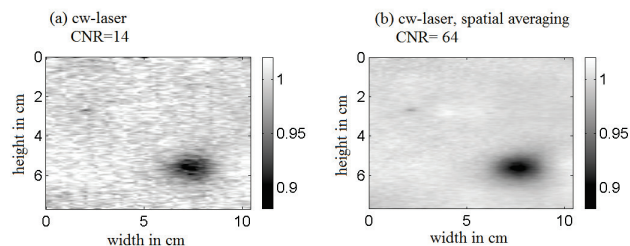


Figure 9. Comparison of cw-laser results (a) with speckle-effect, (b) with reduced speckle-interferences by spatial averaging

The chemical and optical properties of the breast phantom are stable over long periods of time. This allowed us to conduct multiple experiments with different light sources.

Due to the similar results of the high-power LED and the picosecond-pulsed laser, the high-power LED is able to replace the more costly picosecond-pulse-laser in future tests.

Furthermore, our study shows that industrial CCD cameras are suitable detectors.

IV. CONCLUSION

In conclusion, this paper demonstrates that the proposed approach with lineshape light source and camera based detection of diffusely remitted light is feasible. With the current results we can infer that a purely optical recognition of intrinsic absorbing lesions in human tissue will be restricted to a near surface area, if our approach is used. But the actual limits of this approach have yet to be determined. For example, an increase in the local offset will likely increase the possible detection depth. To the best of our knowledge, a recognition depth of 1.5-2 cm seems practical in an assembly of remission.

Future research on the depth resolution of intrinsic absorbers in human tissue can build on the results of this study. One possibility would be the use of established liquid phantoms, which allow adjusting the depth of the lesion continuously. Since high-power LEDs are a cheap and an effective light source for this kind of experiments, we hope that this will enable more research in this area.

Due to the fact that the lesions in the used phantom are considered being realistic models of typical pathological changes in human tissue, the results for in-vivo investigations are expected to be similar.

With this in mind, the results seem to be very promising, since the proposed method has a high potential for medical diagnostic procedures.

REFERENCES

- [1] A. P. Gibson, J .C. Hebden, and S. R. Arridge, "Recent advances in diffuse optical imaging", *Phys. Med. Biol.*, vol. 50, 2005, pp.1-43, Feb. 2005, doi:10.1088/0031-9155/50/4/R01.
- [2] D. Grosenick, H. Rinneberg, R. Cubeddu, and P. Taroni, "Review of optical breast imaging and spectroscopy.," *J. Biomed. Opt.*, vol. 21(9), pp. 091311_1-27, Jul. 2016, doi:10.1117/1.JBO.21.9.091311.
- [3] A. N. Sen, S. P. Gopinath, and C. S. Robertson, "Clinical application of near-infrared spectroscopy in patients with traumatic brain injury: a review of the progress of the field.," *Neurophotonics*, vol. 3(3), pp. 031409_1-5, Jul. 2016, doi:10.1117/1.NPh.3.3.031409.
- [4] G. Greisen, B. Andresen, A. M. Plomgaard, and S. Hyttel-Sørensen, "Cerebral oximetry in preterm infants: an agenda for research with a clear clinical goal.," *Neurophotonics*, vol. 3(3), pp. 031407_1-7, Jul. 2016, doi:10.1117/1.NPh.3.3.031407.
- [5] F. Moreau, R. Yang, V. Nambiar, A. M. Demchuk, and J. F. Dunn, "Near-infrared measurements of brain oxygenation in stroke.," *Neurophotonics*, vol. 3(3), pp. 031403_1-8, Jul. 2016, doi:10.1117/1.NPh.3.3.031403.
- [6] B. Grassi and V. Quaresima, "Near-infrared spectroscopy and skeletal muscle oxidative function in vivo in health and disease: a review from an exercise physiology perspective.," *J. Biomed. Opt.*, vol. 21(9), pp. 091313 1-20, Sep. 2016, doi: 10.1117/1.JBO.21.9.091313.
- [7] G. Hu, Q. Zhang, V. Ivkovic, and G. E. Strangman, "Ambulatory diffuse optical tomography and multimodality physiological monitoring system for muscle and exercise applications.," *J. Biomed. Opt.*, vol. 21(9), pp. 91314ff, Sep. 2016, doi:10.1117/1.JBO.21.9.091314.

- [8] B. Ebert, J. Voigt, R. Macdonald, U. Schneider, A. Thomas, B. Hamm, and K.-G. A. Hermann, "Detection of rheumatoid arthritis using non-specific contrast enhanced fluorescence imaging", *Acad. Radiol.*, vol. 17(3), pp. 375–381, Mar. 2010, doi: 10.1016/j.acra.2009.09.016. Epub 2009 Dec 6.
- [9] X. Intes, J. Ripoll, Y. Chen, S. Nioka, A. G. Yodh, and B. Chance, "In vivo continuous-wave optical breast imaging enhanced with indocyanine green," *Med Phys.*, vol.30(6), pp. 1039-1047, Jun. 2003, doi: 10.1118/1.1573791.
- [10] B. Alacam, B. Yazici, X. Intes, and B. Chance, "Analysis of ICG pharmacokinetics in cancerous tumors using NIR optical methods." *Conf Proc IEEE Eng Med Biol Soc.*, 2005, pp. 62-65, doi: 10.1109/IEMBS.2005.1616342.
- [11] B. Alacam, B. Yazici, X. Intes, S. Nioka, and B. Chance, "Pharmacokinetic-rate images of indocyanine green for breast tumors using near-infrared optical methods," *Phys. Med. Biol.*, vol. 53, pp. 837–859, Jan. 2008, doi:10.1088/0031-9155/53/4/002.
- [12] Y. Tsujino, K. Mizumoto, Y. Matsuzaka, H. Niihara, and E. Morita, "Fluorescence navigation with indocyanine green for detecting sentinel nodes in extramammary Paget's disease and squamous cell carcinoma." *J Dermatol.*, vol. 36(2), pp. 90-94, Feb. 2009, doi: 10.1111/j.1346-8138.2009.00595.x
- [13] A. Hagen, D. Grosenick, R. Macdonald, H. Rinneberg, S. Burock, P. Warnick, A. Poellinger, and P. M. Schlag, "Late-fluorescence mammography assesses tumor capillary permeability and differentiates malignant from benign lesions," *Opt Express.*, vol. 17(19), pp. 17016-17033, Sep. 2009, doi: 10.1364/OE.17.017016
- [14] A. Poellinger, S. Burock, D. Grosenick, A. Hagen, L. Lüdemann, F. Diekmann, F. Engelken, R. Macdonald, H. Rinneberg, and P. M. Schlag, "Breast cancer: early- and late-fluorescence near-infrared imaging with indocyanine green--a preliminary study," *Radiology*, vol. 258(2), pp. 409-416, Feb. 2011, doi: 10.1148/radiol.10100258.
- [15] S. G. Werner, H. Langer, P. Schott, M. Bahner, M. Schwenke, G. Lind-Albrecht, F. Spiecker, B. Kurtz, G. R. Burmester, and M. Backhaus, "Indocyanine green-enhanced fluorescence optical imaging in patients with early and very early arthritis: a comparative study with magnetic resonance imaging." *Arthritis Rheum.*, vol. 65(12), pp. 3036 – 3044, Dec.2013, doi: 10.1002/art.38175.
- [16] V. Ntziachristos and B. Chance, "Probing physiology and molecular function using optical imaging: applications to breast cancer." *Breast Cancer Res.*, vol. 3(1), pp. 41-46, 2001, doi:10.1186/bcr269.
- [17] V. Ntziachristos, A. G. Yodh, M. Schnall, and B. Chance, "Concurrent MRI and diffuse optical tomography of breast after indocyanine green enhancement." *Proc Natl Acad Sci USA.*, vol. 97(6), pp. 2767-2772, Mar 2000, doi: 10.1073/pnas.040570597.
- [18] B. Zhu and E. M. Sevick-Muraca, "A review of performance of near-infrared fluorescence imaging devices used in clinical studies," *The British Journal of Radiology*, vol. 88(1045), pp. 1-26, Dec. 2014, doi: 10.1259/bjr.20140547
- [19] A. Corlu, R. Choe, T. Durduran, M. A. Rosen, M. Schweiger, S. R. Arridge, M. D. Schnall, and A. G. Yodh, "Three-dimensional in vivo fluorescence diffuse optical tomography of breast cancer in humans," *Opt Express.*, vol. 15(11), pp. 6696-6716, May 2007, doi: 10.1364/OE.15.006696.
- [20] D. Grosenick, H. Wabnitz, and B. Ebert, "Review: Recent advances in contrast-enhanced near infrared diffuse optical imaging of diseases using indocyanine green," *J. Near Infrared Spectrosc.*, vol. 20(1), pp. 203–221, Dec. 2011, doi: 10.1255/jnirs.964
- [21] T. J. Muldoon, S. A. Burgess, B. R. Chen, D. Ratner, and E. M. C. Hillman, "Analysis of skin lesions using laminar optical tomography". *Biomed. Opt. Express.*, vol. 3(7), pp. 1701-1712, Jun 2012, doi: 10.1364/BOE.3.001701.
- [22] S. A. Burgess, D. Ratner, B. R. Chen, and E. M. C. Hillman, "Fiber-optic and articulating arm implementations of laminar optical tomography for clinical applications." *Biomed. Opt. Express.*, vol. 1(3), pp. 780-790, Sep. 2010, doi: 10.1364/BOE.1.000780
- [23] R. Freyer, "Development of an optical image giving procedure for the medical diagnostics," („Entwicklung eines optischen Bildgebungsverfahrens zur medizinischen Diagnostik.“) , master thesis HTW Berlin, May 2015, unpublished
- [24] A. Hagen, "Method and device for acquiring optical depth information of an optical scattering object", DE patent DE102015107485B3, (WO002016180404A1), 29. Sep. 2016
- [25] A. Bailleu, A. Hagen, D. Hofmann, "Format-filling digitization of handlarge parts of the body and 3D-Rekonstruktion of the objects for favorable medical application," („Formatfüllende Digitalisierung handgroßer Körperteile und 3D-Rekonstruktion der Objekte zur vorteilhaften medizinischen Anwendung.“) In: *Digitalisierung: Menschen zählen. Beiträge und Positionen der HTW Berlin*, Hg. Matthias Knaut, BWV Berliner Wissenschafts-Verlag, vol. 6, pp. 252-257, Nov. 2016, ISBN 978-3-8305-3700-7
- [26] A. Bailleu, A. Hagen, „3D-Rekonstruktion of handlarge parts of the body with diagnostically relevant depth information in the surface texture,“, („3D-Rekonstruktion handgroßer Körperteile mit diagnostisch relevanten Tiefeninformationen in der Oberflächentextur.“ In: *3D-Nordost*, GfAI, pp. 133-142, Dec.2016, ISBN 978-3-942709-16-3
- [27] P. Azad, T. Gockel, R. Dillmann, "Computer Vision–Principles and Practice," *Elektor International Media*, 2008, ISBN: 978-0905705712 (German: 2007, ISBN: 978-3895761652).